Journal of Statistical Mechanics: Theory and Experiment
An IOP and SISSA journal

Thermodynamics of trajectories of the one-dimensional Ising model

Ernesto S Loscar[1], Antonia S J S Mey and Juan P Garrahan

School of Physics and Astronomy, University of Nottingham, Nottingham NG7 2RD, UK
E-mail: yasser.loscar@gmail.com, ppxasjsm@nottingham.ac.uk and juan.garrahan@nottingham.ac.uk

Received 21 October 2011
Accepted 17 November 2011
Published 16 December 2011

Online at stacks.iop.org/JSTAT/2011/P12011
doi:10.1088/1742-5468/2011/12/P12011

Abstract. We present a numerical study of the dynamics of the one-dimensional Ising model by applying the large-deviation method to describe ensembles of dynamical trajectories. In this approach trajectories are classified according to a dynamical order parameter and the structure of ensembles of trajectories can be understood from the properties of large-deviation functions, which play the role of dynamical free-energies. We consider both Glauber and Kawasaki dynamics, and also the presence of a magnetic field. For Glauber dynamics in the absence of a field we confirm the analytic predictions of Jack and Sollich about the existence of critical dynamical, or space–time, phase transitions at critical values of the 'counting' field s. In the presence of a magnetic field the dynamical phase diagram also displays first order transition surfaces. We discuss how these non-equilibrium transitions in the 1d Ising model relate to the equilibrium ones of the 2d Ising model. For Kawasaki dynamics we find a much simpler dynamical phase structure, with transitions reminiscent of those seen in kinetically constrained models.

Keywords: classical Monte Carlo simulations, classical phase transitions (theory), finite-size scaling, phase diagrams (theory)

[1] Permanent address: Instituto de Investigaciones Fisicoquímicas Teóricas y Aplicadas (INIFTA), UNLP, CCT-La Pata, CONICET, Sucursal 4, CC 16, (1900) La Plata, Argentina.

1742-5468/11/P12011+22$33.00

Contents

1. Introduction

In this paper we perform a detailed numerical study of the trajectories of the one-dimensional Ising model under both Glauber and Kawasaki dynamics. We do so by means of the 'thermodynamics of trajectories' method introduced in [1]–[4], which in turn is based on Ruelle's thermodynamic formalism for dynamical systems [5, 6]. The basic idea is to understand dynamical properties of a many-body system by treating ensembles of trajectories in a way which is analogous to how one understands static or structural properties via the ensemble method for configurations (or microstates) in standard equilibrium statistical mechanics. In order to classify trajectories one defines a suitable dynamical order parameter, one that captures the essence of the physics one is trying to uncover. As we will show below, a convenient one is given by the 'dynamical activity' [2, 3, 7], which for a lattice problem like the ones we study in this paper corresponds to the number of configuration changes (spin flips in our case) in a trajectory. Alternatively, it could be the time integral of a standard observable, such us the time-integral magnetization. One can then study ensembles of trajectories classified by dynamical activity or, more conveniently, as we show below, by their conjugate 'counting' field s. For trajectories observed over long times a large-deviation principle [8] holds such that the distributions of the activity over the ensemble of trajectories, or their corresponding generating functions, are determined by time independent 'large-deviation' functions, which play a role analogous to thermodynamic potentials (entropies or free-energies) for the dynamics. This approach has proved successful recently in uncovering dynamical or 'space–time' phase transitions in a variety of classical many-body systems, most notably glass models, see e.g. [3], [9]–[11]. In these systems the thermodynamics is either trivial, as in kinetically constrained models of glasses [12], or not very revealing, as in more realistic liquid models [13], but the dynamical phase structure is extremely rich, i.e. complex and highly correlated relaxational dynamics can emerge independently of

J. Stat. Mech. (2011) P12011

any form of complex thermodynamics, and this is clearly revealed by the large-deviation method for trajectories.

Therefore a natural question is the following: what is the dynamical phase structure of systems which do display strong thermodynamic features, and is there any relationship between thermodynamic and dynamical, or space–time, phases? Recent work has addressed this issue in certain simple models, including mean-field Ising and Potts models [14] and certain mean-field spin glass models [15, 16]. Specifically, and directly related to the work we present here, there is a recent paper by Jack and Sollich [17] in which they study analytically the dynamical phases of the 1d Ising model with Glauber dynamics. By mapping the problem to that of a quantum Ising model in a transverse field, they managed to obtain the large-deviation function that plays the role of a free-energy for trajectories, and showed that in an enlarged T–s (temperature/counting field) space of parameters there are second order dynamical transitions between active (and paramagnetic) and low-activity (and ferromagnetic) dynamical phases—transitions which are not observed under standard thermodynamic conditions—with critical properties of the classical 2d Ising universality class.

The current paper builds on the results of Jack and Sollich. By means of path sampling methods [18] we generate ensembles of trajectories biased by the counting field s, the so-called s-ensembles [9]. We confirm Jack and Sollich's predictions for the Glauber dynamics in the absence of a magnetic field, providing also detailed analysis of the scaling properties of the dynamical transitions. We also extend the problem to the case of non-zero magnetic field. This allows us to map out in detail the full dynamical phase diagram, revealing a host of first and second order dynamical transitions, and the connection between dynamical and thermodynamical phases. We also consider the case of Kawasaki dynamics and show that the dynamical phase structure in this case is analogous to that of kinetically constrained models of glasses [3, 4].

This paper is structured as follows. First, in section 2, we will introduce the theoretical framework and large-deviation formalism, followed by two main sections. In section 3 the theoretical and computational results of the 1d Ising model using Glauber dynamics are discussed with strong focus on the extension of the phase diagram through an external magnetic field and the resulting scaling behaviour. In section 4 we will look at the dynamic behaviour when applying Kawasaki dynamics. Finally our conclusions are given in section 5.

2. Theory and methodology

The objective of this paper is a computational study of the dynamical processes of a 1d Ising spin chain in the presence and absence of a magnetic field, and within Glauber or Kawasaki dynamics. In order to achieve this, we apply what is referred to as the s-ensemble in the literature [3, 4], which will be briefly reviewed in the following. In order to study the dynamics or time evolution of the system of interest, an appropriate observable capturing the dynamics needs to be defined, as well as a set length of time for which the system is observed. In this way a trajectory or history of the system can be defined with a given length in time t_{obs}. The trajectory is the sequence of configurations, and thus contains information about the instantaneous state of the system at each point in time. Any configurational change in the system gives rise to a dynamic observable. The most

J. Stat. Mech. (2011) P12011

basic one is the number of spin flips in a given trajectory. This is referred to as the activity K [2, 3, 7]. In the thermodynamic Gibbs ensemble the probability of observing a specific configuration is governed by the partition function Z. For the dynamics an equivalent object can be constructed, based on the formalism by Ruelle [5], which gives information about the probability of observing a given trajectory. The dynamic partition function is defined as

$$Z(s, t_{\rm obs}) = \langle {\rm e}^{-sK} \rangle_0, \tag{1}$$

where K is the activity of the system. We are considering path averages, denoted by $\langle\,\rangle_0$, over a set time interval starting at $t = 0$ until a later time $t = t_{\rm obs}$ in an equilibrated system. The parameter s is a biasing or counting field conjugate to K and hence allows subtle control over the ensemble of trajectories. In the context of full counting statistics in electronic transport such parameters are referred as 'counting fields' [19]. They play an equivalent role to that of the inverse temperature β as conjugate field of the energy (or to the magnetic field as a conjugate to the magnetization in a magnetic problem) in the Gibbs ensemble.

In order to give a physical meaning to this space–time analogue of the partition function, the large-deviation formalism is used. Traditionally the thermodynamic limit, as in an infinite system size, is considered. In this case the limit of very large observational time $t_{\rm obs}$ will be considered. Thus the partition function can be written in the form

$$Z(s, t_{\rm obs}) \sim {\rm e}^{t_{\rm obs}\psi(s)}, \tag{2}$$

where the 'large-deviation function' ψ [2, 3, 8] plays the role of a free-energy function for trajectories. The structure of this function provides information about the dynamic phase space behaviour of the system, e.g. its singularities indicate phase transitions in ensembles of trajectories.

In order to analyse the dynamic behaviour we consider a set of time extensive observables, well defined within trajectories, such as the time integrated magnetization or energy for the case of an Ising magnet. If A is one of these observables, its expectation values biased according to the modified path ensemble are given by

$$\langle A \rangle_s = \frac{\langle A {\rm e}^{-sK} \rangle_0}{\langle {\rm e}^{-sK} \rangle_0}. \tag{3}$$

Note that for $s = 0$ the equilibrium expectation is recovered. Hence a set of time intensive variables can be defined, normalized by the choice of observational time and system size N. For example for the intensive activity k we have

$$k(s) = \frac{\langle K \rangle_s}{N t_{\rm obs}}. \tag{4}$$

This leads to a generalization of the susceptibilities associated to this ensemble, which are defined in the usual way

$$\chi_{\mathtt{k}} = \frac{\langle K^2 \rangle_s - \langle K \rangle_s^2}{N t_{\rm obs}}. \tag{5}$$

This will further allow the study of the critical behaviour within the dynamics.

J. Stat. Mech. (2011) P12011

This theoretical framework will be used in order to study a 1d Ising spin chain, on a lattice of size N, under the presence of an external magnetic field. The general Hamiltonian for such a system is given by

$$\mathcal{H} = -J\sum_{i=1}^{N}\sigma_i\sigma_{i+1} - h\sum_{i=1}^{N}\sigma_i, \tag{6}$$

where the spins σ_i take values of 1 or -1, depending on their direction, and $J > 0$ is the coupling constant between first neighbours, and takes a value of 1 for our purposes. The second sum describes the coupling of individual spins to the external magnetic field h. Simulations are made using a Monte Carlo scheme in which periodic boundary conditions are considered for the spatial dimension. As usual, the Monte Carlo time is incremented by one unit when N attempts at spin flips are performed. The trajectory length $t_{\rm obs}$ is predefined. Adjusting the field s will allow biasing towards lower or larger activity and thus samples the tails of the equilibrium distribution. Rather than just running different realizations of the equilibrium distribution, we use an adaptation of transition path sampling (TPS) with s-ensemble biasing [18], similar to the one used to generate s-ensembles in certain glassy models [9, 11]. Once an equilibrium trajectory is produced, this can be used as a blueprint for the next trajectory. As in TPS only part of the original trajectory is used. A shooting point is chosen, from which the system is propagated in time, until the chosen observational time is reached. Then, for the original and new trajectories the activity is calculated, which is the incremental number of spin flips observed within the length of the trajectory. This leads to the acceptance of the newly proposed trajectory according to the standard Metropolis criterion

$$P_{\rm accept} = \min(1, {\rm e}^{-s\Delta K}), \tag{7}$$

where ΔK is the difference in activity between the two trajectories. The employed TPS method allows the generation of trajectories with similar values of K and therefore ensures that new trajectories are likely to be accepted. This method has been employed for the generation of data in this paper in an efficient way.

In terms of the Monte Carlo dynamics used within this work, there were two separate computational studies, one using Glauber dynamics and the other Kawasaki dynamics. The motivation for the use of Glauber dynamics over the generally preferred Metropolis dynamics is theoretical. A recent paper has a theoretical solution for the space–time behaviour of the 1d Ising model with Glauber dynamics, employing an ensemble similar to the s-ensemble presented above [17]. Jack and Sollich refer to this ensemble as the g-ensemble. Rather than biasing towards activity an (integrated) energy bias is introduced, where g is the conjugate field to the energy. Analogously to the s-ensemble a dynamical free-energy $\phi(g)$ can be defined for this ensemble. Only in terms of the Glauber dynamics is a theoretical solution readily available in order to quantify the critical behaviour of the system. Thus, the computational model uses a Glauber acceptance criterion, but for the Kawasaki dynamics the preferred Metropolis criterion will be used. This will be presented in detail in the following two sections.

3. Glauber dynamics

In this section we will present the space–time phase diagram obtained from our computational results using Glauber dynamics. In terms of the evolution of the

J. Stat. Mech. (2011) P12011

Monte Carlo dynamics, the probability of accepting a spin flip is given according to the Glauber acceptance criterion [20]

$$P_{\text{accept}} = \frac{1}{1 + \mathrm{e}^{\beta \Delta E}}, \tag{8}$$

where β is the inverse temperature $\beta = 1/k_{\mathrm{B}}T$ and the Boltzmann constant k_{B} is assumed to be 1.

3.1. The phase diagram

Through the temporal evolution a dynamic phase diagram can be constructed in temperature and biasing field s. In [17] a modified path ensemble equivalent to the discussed s-ensemble is considered. In the g-ensemble, similar to the dynamic free-energy $\psi(s)$ introduced in section 2, the dynamical free-energy $\phi(g)$ of the biased ensemble of trajectories can be obtained using the large deviations of the thermodynamic energy with zero magnetic field. It was further shown that the second derivative of $\phi(g)$ diverges to a line of critical points, which can be shown to belong to the universality class of the 2d Ising model. An equivalence between the activity constrained ensemble (with biased field s) and the energy constrained ensemble (with biased field g) can be established, since for the Ising problem we are considering biasing the energy is akin to biasing in terms of the escape rate of the corresponding continuous-time Markov chain, see, e.g., [4]. In this model, due this equivalence the free-energy of the s-ensemble $\psi(s)$ shares the same critical properties as $\phi(g)$, because the two functions only differ in a regular factor. Therefore the dependence on s and T of the second order critical line is given by the following relationship [17]:

$$s(T) = -\ln\left[\tanh\left(2J/k_{\mathrm{B}}T\right)\right]. \tag{9}$$

Figure 1 shows a schematic representation of the dynamic phase diagram for the Ising chain with Glauber dynamics. This phase diagram is defined in a 3d parameter space depending on the set of variables $\{s, T, h\}$. In particular, the line in figure 1 (a) represents the curve given by equation (9), which is a line of critical points in the plane $h = 0$, dividing this plane into two phases: the paramagnetic phase (for $s < s_{\mathrm{c}}$) and the ferromagnetic phase (for $s > s_{\mathrm{c}}$) [17].

Figure 1(a) also shows a line for zero magnetic field given by isothermal conditions $T = T_0$ (dashed line). As indicated, this line contains a critical point corresponding to $s_{\mathrm{c}} = s(T_0)$ given by equation (9). Figure 1(b) shows the magnetization of the Ising chain as a function of the biasing field s at $T = T_0$. Here the critical point $s = s_{\mathrm{c}}$ separates the ferromagnetic phase for $s > s_{\mathrm{c}}$ with non-zero spontaneous magnetization $m \neq 0$ and the paramagnetic phase for $s < s_{\mathrm{c}}$ with $m = 0$. Tuning the biasing field s, once the critical point is reached, the symmetry of the system is spontaneously broken. The inclusion of the magnetic field in the isothermal behaviour gives rise to a third dimension and therefore the plane $T = T_0$ can be considered as shown in the figure 1(c). Here for $s < s_{\mathrm{c}}$ the magnetic field acts on a paramagnet, while for $s > s_{\mathrm{c}}$ the magnetic field acts on a ferromagnet. Figures 1(b) and (c) are analogous to those of the 2d Ising model by assuming $s \to \beta$. In fact by taking $s = s_{\mathrm{c}}$ and using the temperature T (instead of s) as the control parameter, the critical behaviour is in complete analogy with the 2d Ising model. In the presence of an external magnetic field h we expect the system to exhibit

J. Stat. Mech. (2011) P12011

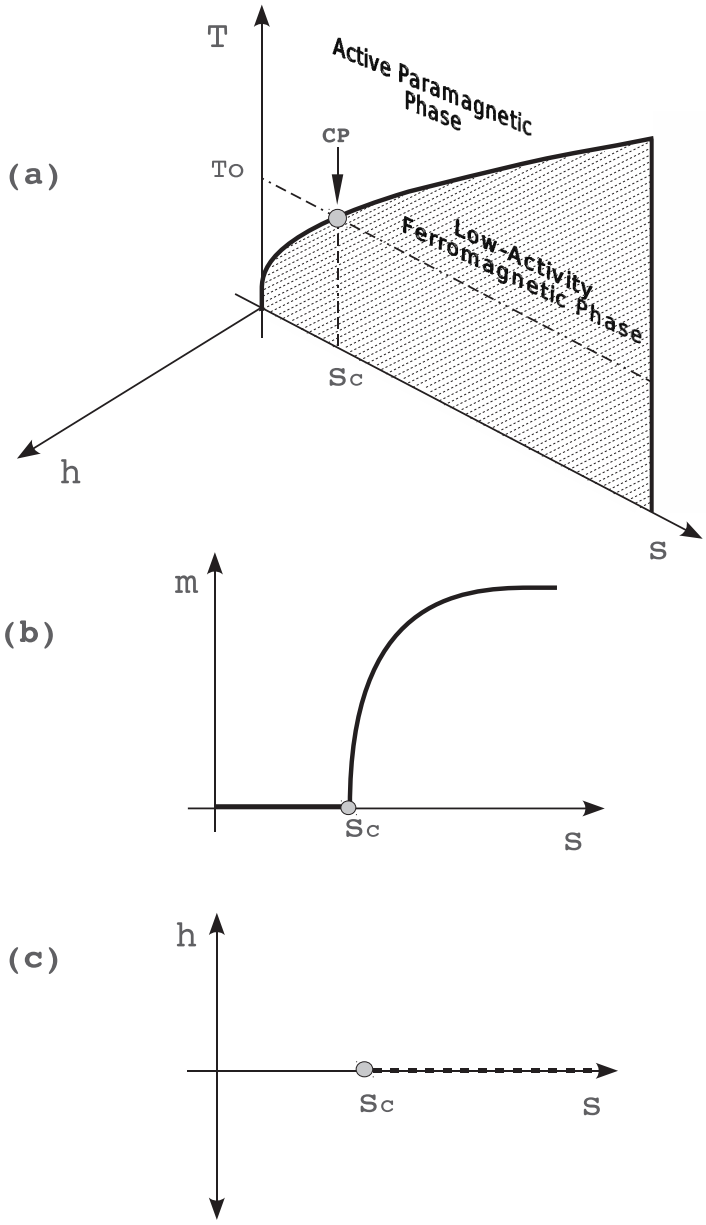

Figure 1. Schematic representation of the phase diagram of the Glauber 1d Ising model in the s-ensemble with magnetic field h. (a) The phase space is defined through three variables T, s, and h. Here the continuous line, into the plane $h = 0$, represents the critical points given by the theoretical solution in [17] separating paramagnetic (and active) and ferromagnetic (and low-activity) dynamical phases. The dashed line corresponds to the conditions $T = T_0 = \text{const}$ and $h = 0$ and contains a critical point (CP) marked by a circle. (b) Spontaneous magnetization as a function of s at temperature $T = T_0$ and $h = 0$ (dashed line drawn in (a)). The symmetry is broken by the biasing field s for $s > s_c$ just at the critical point $s = s_c$. (c) The plane h, s taking $T = T_0$. The critical point $s = s_c$ divides the line into two phases, a paramagnetic phase for $s < s_c$ and a ferromagnetic phase for $s > s_c$. For $s > s_c$, the dashed line represents expected points of first order transitions.

J. Stat. Mech. (2011) P12011

a first order phase transition along the dashed line shown in figure 1(c) where $s > s_c$. This obviously gives rise to an entire surface of critical points for $h = 0$ below the curve of $s(T)$ as shown in figure 1(a). In the following, the second order critical behaviour as predicted by the theory of equation (9) will be studied through Monte Carlo simulations as well as the validity of the existence of the first order surface by means of the presence of an external magnetic field.

3.2. Dynamical continuous phase transition

In this section we study by means of Monte Carlo simulation the critical behaviour of the critical points given by equation (9). As was established in the discussion of section 3.1 describing figure 1, we can use an s-fixed curve or an isothermal in order to reach the critical point. Trajectories are generated as described in section 2 using a fixed temperature T and with zero magnetic field. From each accepted trajectory, of a given value of the biasing parameter s, the set of time extensive variables is obtained. These are the activity K as the number of changes of configuration, the integrated energy $E = \int_0^{t_{\rm obs}} \mathrm{d}t'\, u(t')$, and the integrated magnetization $M = \int_0^{t_{\rm obs}} \mathrm{d}t'\, m(t')$, where $m(t) = \sum_{i=1}^{N} \sigma_i(t)$.

In order to study the critical properties, we need to apply the finite size scaling theory. This is a commonly used technique in computational physics [21]. As we are investigating the scaling behaviour of dynamic properties, the temporal size is given by the observational time $t_{\rm obs}$. In fact, we can see from the definition given by equation (2) that it is analogous to the spatial system size when the equilibrium thermodynamic free-energy is defined. Of course, in our simulations we have to use a system with finite spatial size, i.e. the number of spins N. We have observed that the behaviour of the system is very sensitive with respect to the length of the trajectories $t_{\rm obs}$ (much more than to the length N of the chain). In order to have a consistent analysis of the finite size effects, we have chosen to study the behaviour considering $t_{\rm obs}$ as the scaling parameter, so that the lattice size N is set to a fixed value.

It is worth mentioning that the dynamic evolution of the this system can be described with a time evolution operator, which is equivalent to a quantum Hamiltonian. From this point of view the length ($t_{\rm obs}$) of the trajectories is equivalent to the inverse of the temperature $T^{(\mathrm{q})}$, as in the associated quantum problem discussed in [17] (so that $t_{\rm obs} \leftrightarrow 1/T^{(\mathrm{q})}$). It is well known that there is a mapping between the classical 2d Ising model and the quantum Ising chain [22]. From this mapping we know that the inverse of $T^{(\mathrm{q})}$ is equivalent to the size in one spatial direction in the 2d Ising model (that is $1/T^{(\mathrm{q})} \leftrightarrow L$). Therefore we conclude that $t_{\rm obs}$ in our problem is equivalent to a linear size L in the classical 2d Ising model (i.e. $t_{\rm obs} \leftrightarrow L$). According to this we assume that the finite size effects are given by the same well known relationships used for the thermodynamic 2d Ising model, where we now replace L with $t_{\rm obs}$.

To determinate the critical temperature of a continuous phase transition we can use the peak of the susceptibilities. According to the previous discussion we expect that the susceptibilities have scaling forms given by [21]

$$\chi(t_{\rm obs}) = t_{\rm obs}^{\alpha/\nu} f\left((T - T_c) t_{\rm obs}^{1/\nu}\right), \tag{10}$$

where α is the exponent that characterizes the divergence of the susceptibility χ and ν

J. Stat. Mech. (2011) P12011

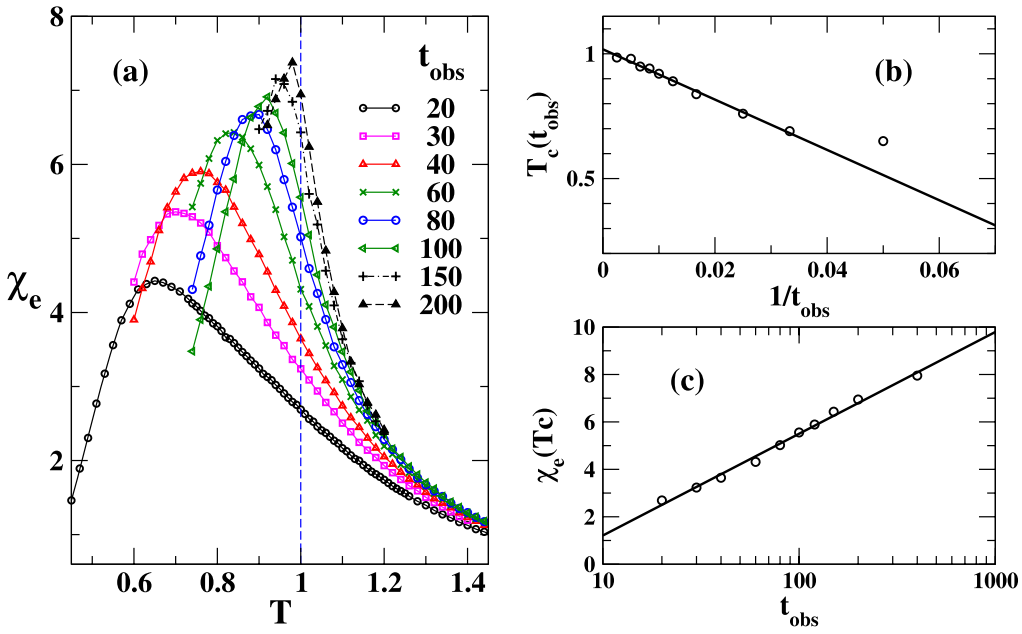

Figure 2. (a) Susceptibility of the energy as a function of T at constant $s = 0.036\ 635\ 37$. The vertical dashed line corresponds to $T_c = 1.00$ given by equation (9). (b) Effective critical T, taken as the T at the peak of (a), against $1/t_{obs}$. The extrapolated value, for $t_{obs} \to \infty$, is $T_c = 1.02 \pm 0.02$. (c) Susceptibility at $T_c = 1.00$ versus t_{obs}. The divergence is logarithmic, as in the case of the specific heat in the 2d Ising model.

is the length correlation exponent. Furthermore, the locations of the peaks define an effective size-dependent transition temperature which is expected to vary as

$$T_c(t_{obs}) = T_c(\infty) + A t_{obs}^{-1/\nu}. \tag{11}$$

As is shown in figure 1, we can use an s-fixed curve or an isothermal one in order to reach the critical point, and therefore the scaling given by equation (11) is expected in terms of T or in terms of s, respectively.

Figure 2 shows the simulation results for a fixed value of s and varying the temperature T. We have chosen the value of s as $s_c = 0.036\,635\,37$, which corresponds to s_c at $s(T \equiv 1)$ as given by equation (9). We define the generalized susceptibility of the energy χ_e by means of

$$\chi_e = \frac{\langle E^2 \rangle_s - \langle E \rangle_s^2}{T^2 N t_{obs}}. \tag{12}$$

In figure 2(a) we plot χ_e as a function of the temperatures and for different trajectory lengths t_{obs}. We used a lattice size $N = 64$, and the averages were taken over 5×10^6 realizations of single trajectories. Peaks close the critical point are clearly observed, which sharpen as the system size is increased (i.e. t_{obs}). We have used the locations of these peaks as the definition of a size-effective 'critical temperature' $T_c(t_{obs})$.

Figure 2(b) shows the effective critical temperature as a function of the inverse of the trajectory length t_{obs}. We can see that the behaviour is compatible with equation (11)

J. Stat. Mech. (2011) P12011

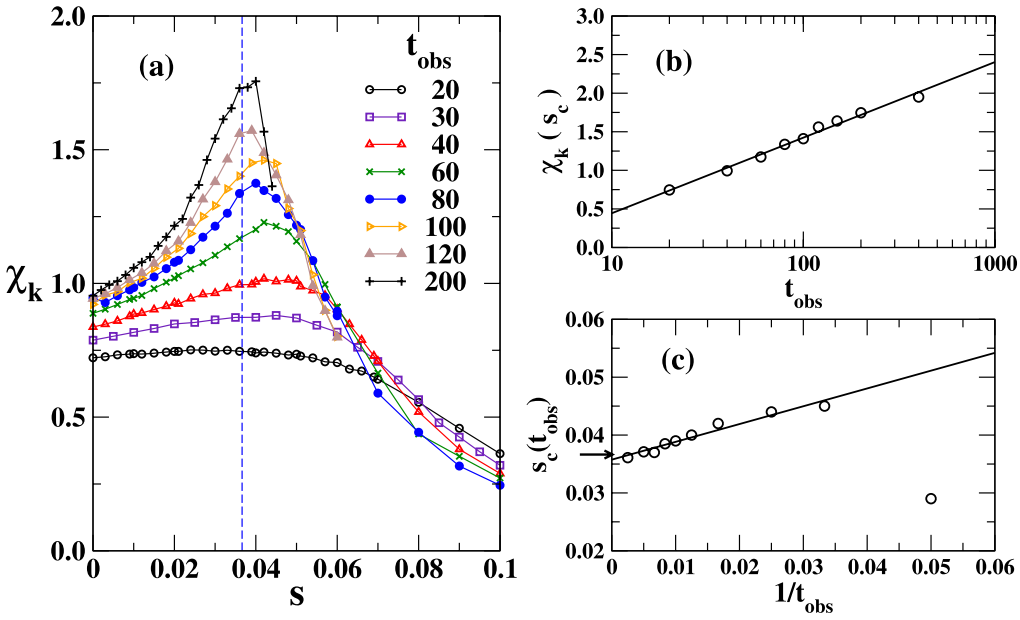

Figure 3. (a) Susceptibility of the activity as a function of s at constant temperature $T = 1$. The vertical dashed line corresponds to $s = s_c = 0.036\,635\,37$ given by equation (9). (b) Susceptibility at $s = s_c = 0.036\,635\,37$ constant versus t_{obs}. The critical divergence of the χ_k is logarithmic. (c) Convergence of the effective critical s, taken as the value of s where the susceptibility peaks in part (a) as a function of t_{obs}. The extrapolated value, for $t_{obs} \to \infty$, is $s_c = 0.036 \pm 0.001$. The arrow indicates the theoretical value from equation (9).

taking an exponent $\nu = 1$ corresponding to the 2d Ising universality class. The continuous line is given by the linear fit of the data. From this our extrapolated estimated value for the critical temperature is $T_c = 1.02 \pm 0.02$, and it is consistent with the theoretical value given by equation (9). Also, figure 2(c) shows the value of the susceptibility measured in figure 2(a) for $T = T_c = 1$ and different sizes in log-linear scale.

As the dynamical free-energy $\phi(g)$ must have the same critical properties as the thermodynamic free-energy $f(T)$ of the 2d Ising model, its second derivative must be analogous to the behaviour of the specific heat. In fact it can be shown that the second derivative of $\phi(g)$ has a logarithmic divergence when the critical point is approximated [17]. Figure 2(c) shows that a logarithmic behaviour is observed, which means that equation (10) holds with an exponent $\alpha = 0$, as discussed above.

As we have already indicated, the critical behaviour can also be accessed by choosing a constant temperature T_0 and considering different values of the biasing field s. In figure 3(a) we plot the susceptibility of the activity χ_k, given by the equation (5), versus s with fixed $T = 1$. The observed behaviour is analogous to the energy fluctuations. Again the value of the critical s_c can be extrapolated making use of equation (11), but in this case using the biasing field s instead of T. In figure 3(b) we plot the effective critical s and the linear fit gives us an estimate of the critical field, that is $s_c = 0.036 \pm 0.01$. Once again this result is consistent with $\nu = 1$. Also figure 3(c) shows the susceptibility χ_k for $s = 0.036\,635\,37$ in a log-linear scale. We observe again that equation (10) is valid with a logarithmic divergence of the susceptibility of the activity, which means that $\alpha = 0$.

J. Stat. Mech. (2011) P12011

So far a complete equivalence in the critical behaviour between the biasing field s and the inverse of the temperature $1/T$ is observed. Also, similar results are obtained when studying finite size effects of the fluctuations of K (or E) with respect to T (or s).

Let us now consider the system in the presence of an external magnetic field h, which couples to the spins of the chain according to equation (6). We have studied the Ising Glauber chain with the magnetic field h close to the critical point.

We remark that the magnetic susceptibility of the 2d Ising model is given by

$$\chi_{\mathrm{T}} = \frac{\langle m^2\rangle - \langle m\rangle^2}{kTN} = \frac{1}{kTN}\sum_{i,j=1}^{N} G(r_i, r_j), \tag{13}$$

where $G(r_i, r_j) = \langle\sigma_i\sigma_j\rangle - \langle\sigma_i\rangle\langle\sigma_j\rangle$ is the two point correlation function, so that χ_{T} is static, and is a measure of the spatial correlations. In the critical isotherm, the magnetic susceptibility shows a critical divergence given by

$$\chi_{\mathrm{T}} \propto h^{-(1-1/\delta)}. \tag{14}$$

As the critical exponent is $\delta = 15$, thus $1 - 1/\delta = 14/15 \approx 0.933$.

Following the definition of the generalized dynamic susceptibilities, we define the time-spatial magnetic susceptibilities as

$$\chi_{\mathtt{m}} = \frac{\langle M^2\rangle - \langle M\rangle^2}{kTNt_{\mathrm{obs}}} = \frac{1}{kTNt_{\mathrm{obs}}}\sum_{i,j=1}^{N}\int_0^{t_{\mathrm{obs}}}\int_0^{t_{\mathrm{obs}}} \mathrm{d}t''\,\mathrm{d}t'\,G(r_i, r_j, t', t''), \tag{15}$$

where now $G(r_i, r_j, t', t'') = \langle\sigma_i(t')\sigma_j(t'')\rangle_s - \langle\sigma_i(t')\rangle_s\langle\sigma_j(t'')\rangle_s$ is the two point and two time correlation function. This susceptibility ($\chi_{\mathtt{m}}$) has both spatial and temporal correlations. We can also define in the s-ensemble the static (or instantaneous) susceptibility in the same way as in equation (13), which is given by

$$\chi_{\mathrm{T}}^{(s)} = \frac{\langle m^2\rangle_s - \langle m\rangle_s^2}{kTN} = \frac{1}{kTN}\sum_{i,j=1}^{N} G(r_i, r_j, \tau = 0), \tag{16}$$

where we have introduced $\tau \equiv |t'' - t'|$.

We can apply the schema used for standard critical phenomena given by the dynamic scaling hypothesis, and obtain a relationship between the critical exponents corresponding to these susceptibilities [23]. So, in the thermodynamics limit, assuming a translational and temporal invariant correlation function G, and the existence of a diverging correlation length ξ, we obtain

$$\chi_{\mathrm{T}}^{(s)} \propto \sum_{R} G(R, 0) \propto \xi^{2-\eta}, \tag{17}$$

and

$$\chi_{\mathtt{m}} \propto \sum_{R}\int \mathrm{d}\tau'\,G(R, \tau') \propto \xi^{2-\eta}\xi^{z}, \tag{18}$$

where we have introduced $R \equiv |r_i - r_j|$. Here z is the dynamical critical exponent. For our

J. Stat. Mech. (2011) P12011

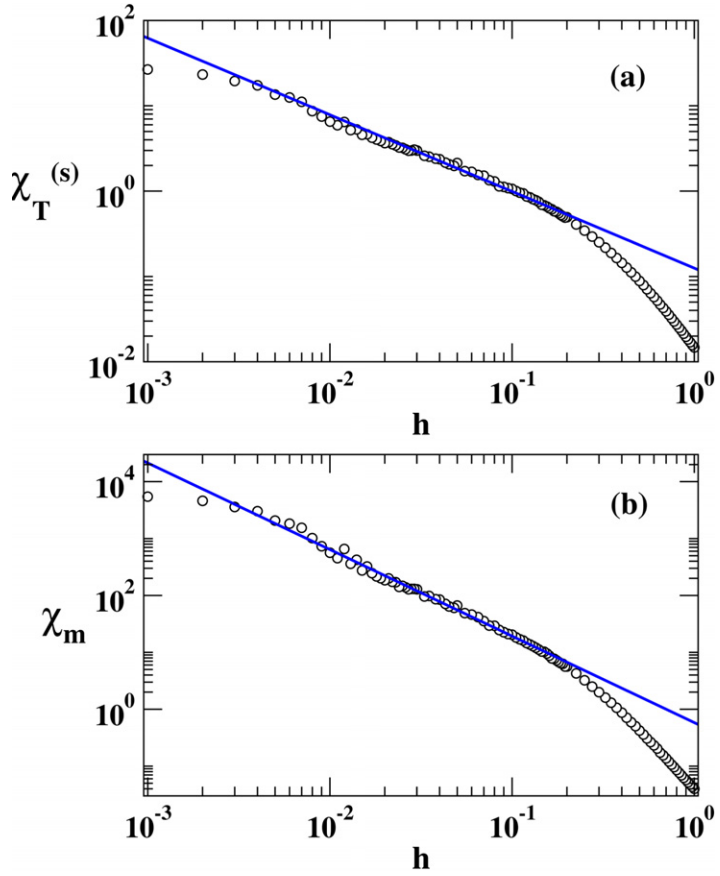

Figure 4. (a) Susceptibility of the instantaneous magnetization corresponding to spatial fluctuations. The continuous line is a fit of a power law that gives an exponent 0.90 ± 0.05, in good agreement with the exponent of the magnetic susceptibility of the 2d Ising model $1 - 1/\delta \approx 0.933$. (b) Susceptibility of the integrated magnetization corresponding to spatio-temporal fluctuations. The continuous line is a fit of a power law that gives an exponent 1.50 ± 0.05.

system we have taken $T = T_c$, that is the critical isotherm, at constant $s = s_c$. Therefore the length correlation diverges according to the magnetic field. By assuming the usual Ising behaviour [24], we have

$$\xi \propto |h|^{-\Theta}, \qquad \text{with } \Theta = \nu(\beta + \gamma)^{-1}. \tag{19}$$

From equations (17) and (19) we recover the static result $\chi_T^{(s)} \propto h^{-(1-1/\delta)}$, whilst from equations (18) and (19), we find the dynamical critical behaviour given by

$$\chi_m \propto h^{-\Delta}, \qquad \text{with } \Delta = (\gamma + \nu z)(\beta\delta)^{-1}. \tag{20}$$

Figure 4 shows the results of the Monte Carlo simulation of the Ising chain with a magnetic field for 5×10^6 generated trajectories ($N = 64$ and $t_{obs} = 300$). A clear behaviour emerges for external fields of moderate intensity, that is $0.004 \lesssim h$. We have found that the results for different times $t_{obs} = 160, 200, 300$ (and for different numbers of spins $N = 64, 100$) are the same within error bars. For these values of the magnetic field

there are no finite size effects. The stationary thermodynamic behaviour is observed. In other words, for weak field $h \lesssim 0.004$, finite size effects are observed, caused by limited $t_{\rm obs}$ and lattice size N. Any attempt to study the phase space region with a small external field ($h \lesssim 0.004$) would require extensive simulation efforts which are beyond the scope of this paper.

Figure 4(a) shows the *static* susceptibility $\chi_{\rm T}^{(s)}$. We can see that a power law fits in the region of the magnetic field, $0.004 \lesssim h \lesssim 0.2$, with a fitted exponent 0.90 ± 0.05. For higher field ($0.2 \lesssim h$) there is a deviation of the power law regime, as expected far from the critical point. This value is consistent with the value of the 2d Ising model given by equation (14). On the other hand, figure 4(b) shows the susceptibility $\chi_{\rm m}$. The behaviour of the static susceptibility is qualitatively analogous to $\chi_{\rm m}$. However the power law fit within the same region of the magnetic field, $0.004 \lesssim h \lesssim 0.2$, gives a different exponent, that is $\Delta = 1.50 \pm 0.05$. Using the relationship given by equation (20) and assuming the Ising universality, we can conclude that our simulation gives us an estimation of the dynamical critical exponent, which is $z = 1.06 \pm 0.09$. This value is compatible with $z = 1$.

This result shows that through the application of the magnetic field to the Ising chain using the s-ensemble, the spatial correlations involved are similar to those present in the 2d Ising model with field near the critical point, while the response of the integrated magnetization is governed by a (greater) exponent dependent on the dynamical exponent z.

In the system presented here, the static criticality of the 2d Ising model universality class appears in different ways. For the energy and activity criticality arises in the space–time plane (see figures 2 and 3) and is uncovered by means of finite size effects, whereas for simulations with external magnetic field it appears only in the spatial axis (see figure 4(a)) and in the thermodynamic limit.

3.3. Dynamical first order transition

We argued in section 3.1 that in the presence of an external field, the spontaneous broken symmetry should give rise to a first order phase transition in the ferromagnetic phase. So that, for isothermal conditions, a first order phase transition is expected for the biasing field s greater than the critical value $s_{\rm c}(T_0)$ (see figure 1(c)). Illustrating the dynamic behaviour, including an external magnetic field analytically, is non-trivial. This is due to the fact that the mapping of the master equation onto the quantum problem will give rise to highly nonlinear terms. In the following we will address this problem numerically.

We consider the parameter space $\{s, T, h\}$ with focus on an isothermal plane ($T = 1$). In the $h = 0$ plane, two phases are present: a paramagnetic phase for $s < s_{\rm c} \approx 0.037$, and for $s > s_{\rm c} \approx 0.037$ a ferromagnetic phase, as depicted in the schematic of figure 1. Figure 5 shows the results of the Monte Carlo simulations including an external magnetic field, that is the magnetization in terms of h for different values of the biasing field s. In this case we have used a system of $N = 200$ spins, and we generated 10^6 trajectories. In figure 5(a) a smooth curve $m(h)$, in the vicinity of $h = 0$, for a low biasing field $s = 0.02$ can be seen, this is the paramagnetic phase. Meanwhile, figure 5(c) shows a sharp transition, at $h = 0$, for a supercritical value of biasing the field $s = 0.05$, this is the ferromagnetic phase. For completeness, figure 5(b) illustrates the behaviour at the

J. Stat. Mech. (2011) P12011

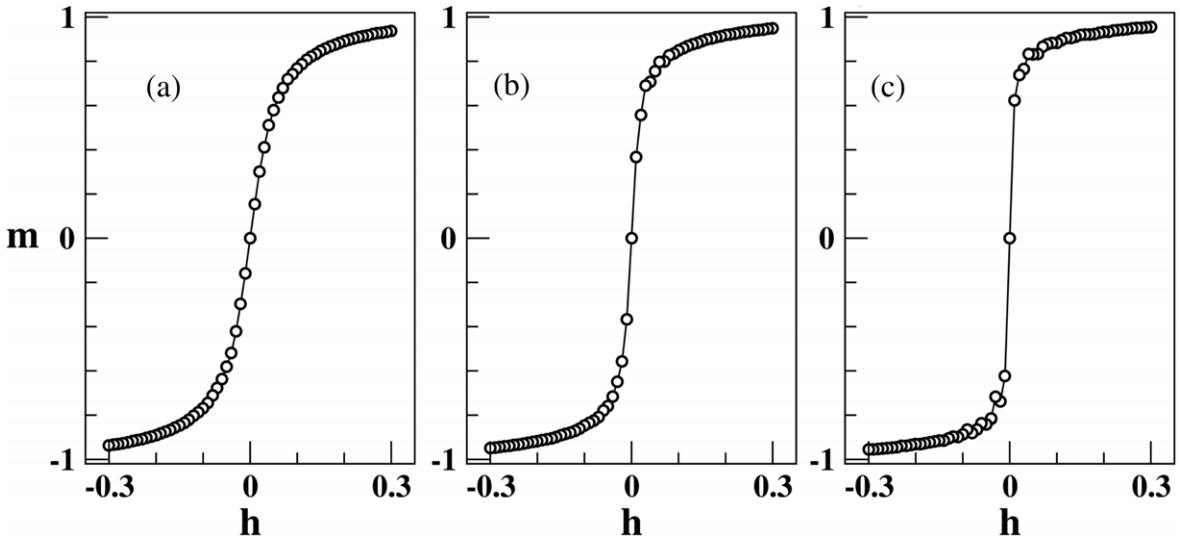

Figure 5. Stationary results for the magnetization of the Ising chain with magnetic field using the s-ensemble for different values of the constant biasing field s. The temperature T is constant ($T = 1$): (a) magnetization for the subcritical behaviour, that is in the paramagnetic phase $s = 0.02 < s_c$; (b) results for the critical value of $s = s_c = 0.036\,635\,37$; and (c) results obtained for the supercritical behaviour, that is in the ferromagnetic phase $s = 0.05 > s_c$.

critical point $s_c = 0.036\,635\,37$. The behaviour of s is equivalent to that of the inverse temperature β for the thermodynamic fluctuations of the Ising ferromagnet. Therefore, we expect that the field-driven first order phase transition ends at the critical point $s = s_c$ ($T = 1, h = 0$) which is the limit of the ferromagnetic phase ($s > s_c$).

In order to capture this behaviour further, hysteretic loops were studied. The simulations were started from a representative trajectory of the stationary distribution, then the external field was perturbed by $h \pm \Delta h$ (with $\Delta h \sim 0.01$). In order to reach a stationary state for the new value of h, n_{relax} steps in the TPS algorithm are taken for equilibration. Then measurements of the observables are taken for n_{obs} steps. Figure 6 shows the resulting loops of the magnetization versus the magnetic field. We used a system size $N = 200$ and $n_{\mathrm{relax}} = 10^2$ TPS moves were attempted, in order to achieve relaxation, and the hysteresis was studied using $n_{\mathrm{obs}} = 10^5$ realizations.

The top panel of figure 6 depicts the hysteresis loop with increasing supercritical s with a trajectory length of $t_{\mathrm{obs}} = 60$, that is $s = 0.05$ for (a), $s = 0.07$ for (b), and $s = 0.08$ for (c). The bottom panel of figure 6 again shows the hysteresis loops, but in this case the observational time of the trajectory was increased to $t_{\mathrm{obs}} = 80$. The values for s are retained ($s = 0.05$ for (d), $s = 0.07$ for (e), and $s = 0.08$ for (f)). Clearly, the areas of the loops increase with t_{obs} as well as with s. This is because as s increases the metastability of the system increases, therefore the loop area also increases. The behaviour with respect to t_{obs} can be treated in terms of an increase in volume, which means the relaxation is slower and therefore an increased loop size is observed. This behaviour supports the idea that the dashed line in figure 1(c) and the surface below the continuous line in figure 1(a) are made of first order phase transition points.

J. Stat. Mech. (2011) P12011

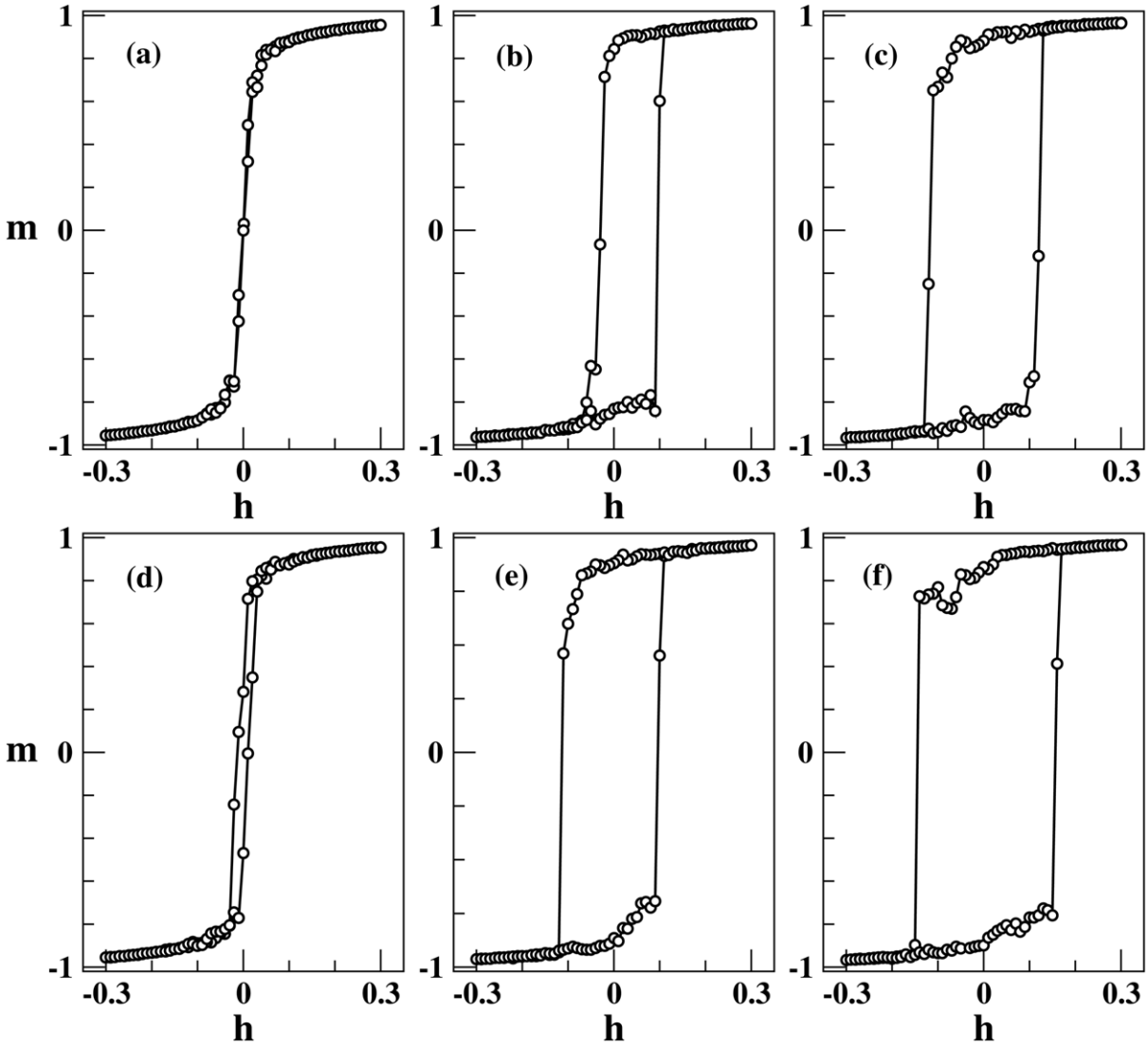

Figure 6. Magnetization versus the magnetic field in the form of hysteresis loops at constant temperature $T = 1$ around the first order transition at $h = 0$. The biasing field s is also fixed (in all cases at supercritical values): for (a) and (d) $s = 0.05$, for (b) and (e) $s = 0.07$, and for (c) and (f) $s = 0.08$. In the top (bottom) panel we have used an observational time $t_{\rm obs} = 60$ ($t_{\rm obs} = 80$). The areas of the loops increase with $t_{\rm obs}$, and with s. More details are given in the text.

4. Kawasaki dynamics

So far we have looked at dynamical models with non-conserved magnetization [14, 17], which in the case of the classic thermodynamics would serve as an order parameter. These are A type models or non-conserved order parameter [25]. In the particular case of the Glauber dynamics it has been shown, and we have verified that, in the dynamic exploration of this model, a line of critical points in the phase space can be found. We expect this kind of behaviour for model A type dynamics.

J. Stat. Mech. (2011) P12011

On other hand, it is interesting to ask about the role of the underlying dynamics on the observed *dynamical* phase diagram. In order to illuminate this point, let us now consider a model belonging to the second class of dynamics, where the magnetization is conserved (conserved order parameter). We have realized Monte Carlo simulations using Kawasaki dynamics. This dynamics conserves the overall magnetization and consists of exchanging neighbouring spins, rather than flipping them. The acceptance function for undergoing a spin exchange is chosen to be the Metropolis criterion

$$P_{\text{accept}} = \text{Min}(1, \text{e}^{-\Delta E/k_{\text{B}}T}), \tag{21}$$

where ΔE is the increment in the energy due to the exchange.

In figure 7 we show the results of the Monte Carlo simulations using the s-ensemble with Kawasaki dynamics for the Ising chain. These simulations were realized at constant temperature $T = 3$ for a spin chain of size $N = 64$ and zero magnetization, i.e. equal populations of spins up and down. Figures 7(a) and (b) show the activity and the susceptibility of the activity, given by equation (5), respectively, versus the biasing field s for different t_{obs}. For low values of s we can observe an active phase which becomes inactive for higher values of s. Also, when the observational time is increased, the jump becomes more abrupt and consequently its susceptibility shows an increasingly sharp peak. Again this is the sign of a phase transition and suggests a good finite size scaling behaviour through increasing the length scale, i.e. t_{obs}, in the same way as was done in section 3.

Figure 8 shows the behaviour of the integrated energy with respect to s and its susceptibility defined by equation (12). This behaviour is qualitatively the same as the behaviour of the activity. We can understand this similarity qualitatively. The energy is proportional to the number of domain walls (that is the number of neighbouring spins pointing in opposite directions). Using the Kawasaki dynamics we require two neighbouring sites with different spins in order to make a spin flip, thus the same factor governs both the energy and the activity.

Figures 7 and 8 suggest that the observed transitions are first order transitions. Generally finite size scaling of a first order transition [21] predicts scaling in terms of the volume $V = L^D$. According to this theory, for a finite volume V, we can define an effective critical point s_{c} as the value of s at which the susceptibilities have the maximum $\chi^{\max}$. In this way, the following scaling behaviour is expected:

$$s_{\text{c}}(t_{\text{obs}}) = s_{\text{c}}^{(\infty)} + AV^{-1}, \tag{22}$$

where $s_{\text{c}}^{(\infty)}$ is the thermodynamic limit $s_{\text{c}}(t_{\text{obs}} \to \infty)$, and

$$\chi^{\max} \propto V. \tag{23}$$

In our case, the volume in the space–time is given by $V = Nt_{\text{obs}}$. By fixing the number of spins N, we can write out $V = t_{\text{obs}}$ in equations (22) and (23).

Figure 9 illustrates that the finite size analysis holds for the activity (the same behaviour is also observed for the energy). In figure 9(a) the location s_{c} of the maximum χ_{k} is plotted for two Ising chains of lengths $N = 64$ and 100 against t_{obs}^{-1}. The effective critical value s_{c} decreases with increasing t_{obs} and with increasing N. Using equation (22) to calculate the extrapolated value to $t_{\text{obs}} \to \infty$ we obtain the values $s_{\text{c}} = 0.003 \pm 0.001$ for $N = 64$, and $s_{\text{c}} = 0.001 \pm 0.001$ for $N = 100$ (the same results are obtained from the energy analysis).

J. Stat. Mech. (2011) P12011

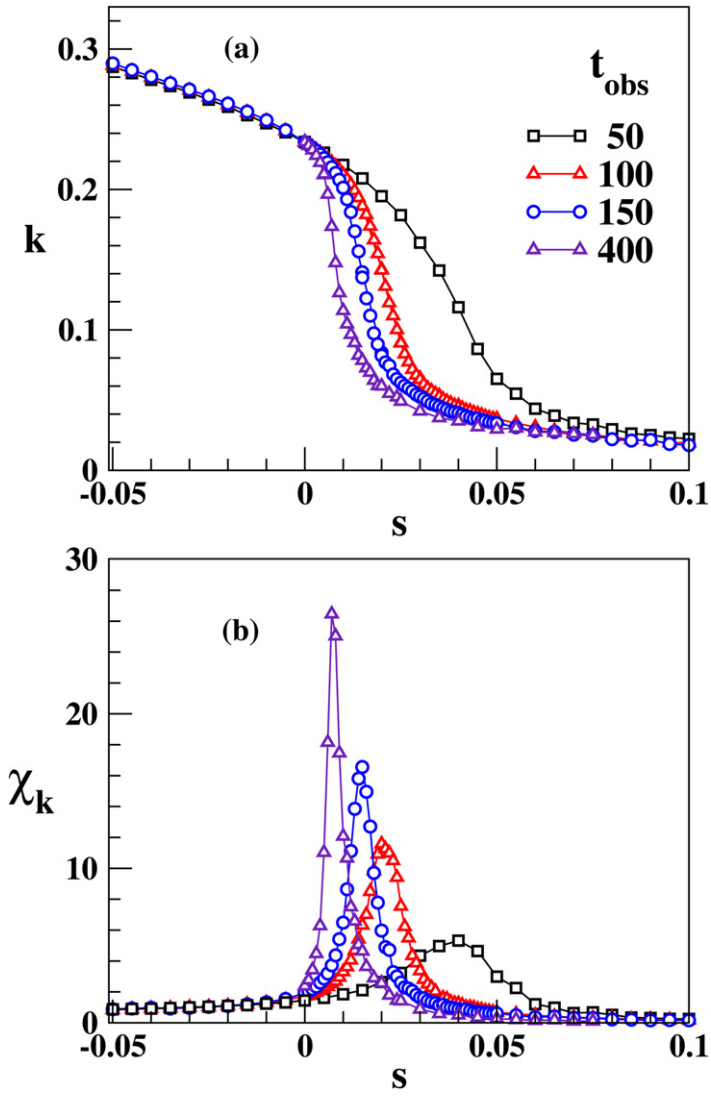

Figure 7. Results of the Monte Carlo simulations using the s-ensemble with Kawasaki dynamics taking the temperature constant ($T = 3$). When the observational time $t_{\rm obs}$ is varied, as indicated in (a), finite size effects are observed. (a) Activity versus the biasing field s. (b) Susceptibility of the activity as a function of s.

Figure 9(b) shows the heights of the peaks drawn from the susceptibility of the activity versus the observational time. The continuous line in this figure is a power law given by equation (23). For the smaller system size the power law is not observed at all. For the larger size we can see that there is a narrow region, for intermediate values of $t_{\rm obs}$, where the power law holds. These results show that for small $t_{\rm obs}$ there are boundary effects in the times of the trajectories, and for longer $t_{\rm obs}$ there are boundary effects in the space of the spin chain. These rounding effects make it difficult to observe the scaling behaviour given by equation (23) for the sizes and observational times used in this paper.

The previous analysis of figures 9(a) and (b) indicates a first order phase transition, between an active phase (for s negative) and an inactive phase (for s positive), and a

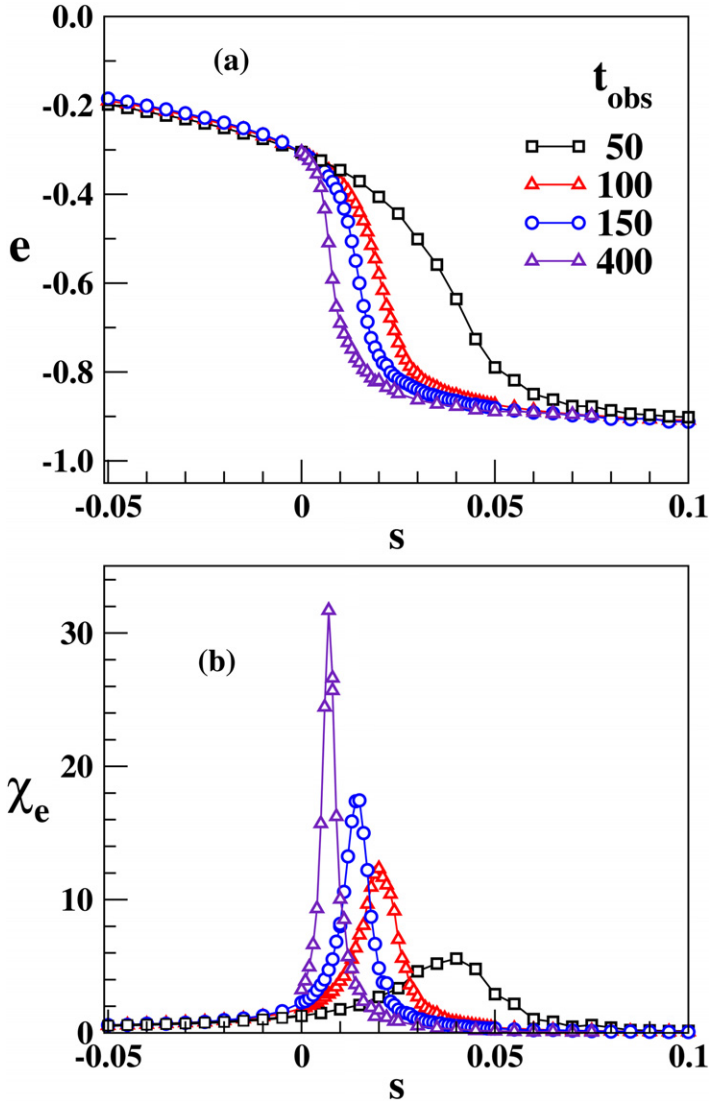

Figure 8. Results of the Monte Carlo simulations using the s-ensemble with Kawasaki dynamics taking the temperature constant ($T = 3$). When the observational time $t_{\rm obs}$ is varied, as indicated in (a), finite size effects are observed. (a) Energy versus the biasing field s. (b) Susceptibility of the energy as a function of s.

transition point at $s_{\rm c} = 0$. This space–time phase structure, of coexistence of active and inactive dynamical phases at $s = 0$, is similar to that of idealized kinetically constrained models [3, 4].

It is worth mentioning that the activity and the energy, in the inactive phase (see figures 7(a) and 8(a)), are $\sim 1/N$ due to finite size effects. In fact the dynamics implies that there always are at least two domain walls, which separate the up and down pointing spin domains in order to conserve zero magnetization. Because of this constraint the minimum of the energy per site is given by $e - e_0 = 2/N$, where e_0 is the unconstrained energy corresponding to the ground state. For increasing N and increasing $t_{\rm obs}$ the energy

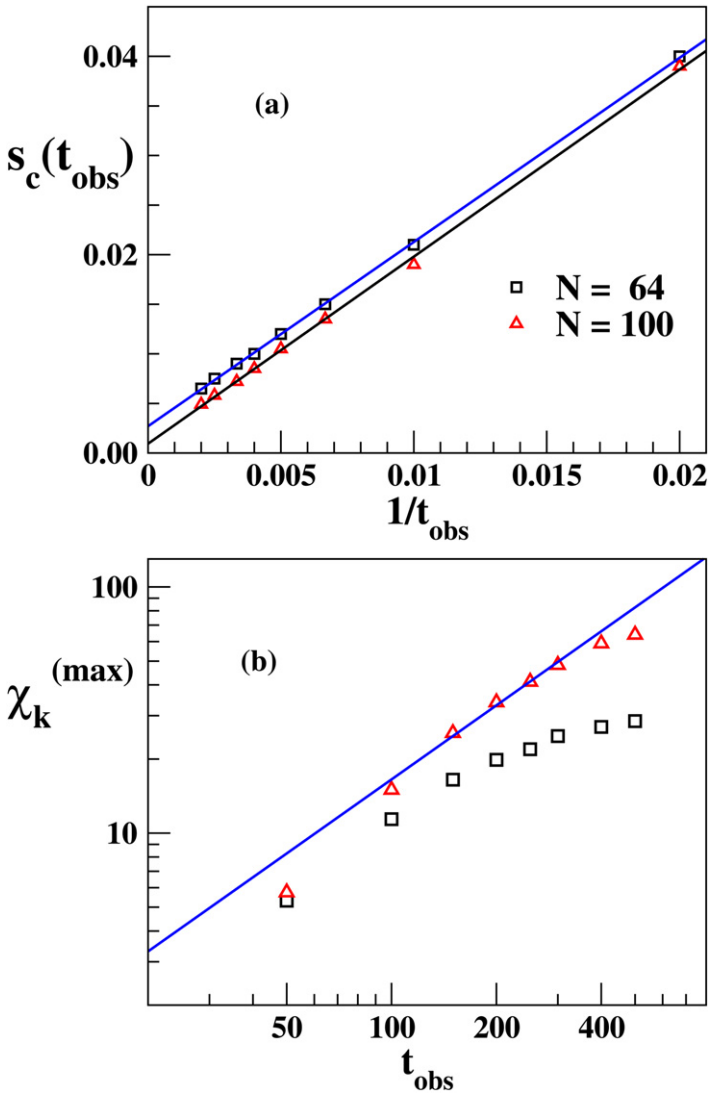

Figure 9. Results of the Monte Carlo simulations using the s-ensemble with Kawasaki dynamics taking the temperature constant ($T = 3$). The black squares are results obtained from the data of figure 7 for $N = 64$. For comparison, the red triangles are data obtained from simulations with $N = 100$ analogous to figure 7 (data not shown for the sake of clarity). (a) The effective critical biasing field s_c, defined as the location of the peak in the susceptibility χ_k, as a function of $1/t_{obs}$. The straight lines are fits used for the extrapolations of s_c to the limit $t_{obs} \to \infty$ by means of the scaling valid for first order transitions given by equation (22). The result is $s_c = 0.003 \pm 0.001$ ($s_c = 0.001 \pm 0.001$) for $N = 64$ ($N = 100$). (b) Height of the peak of the susceptibilities of the activity for the same cases as in (a). The straight line is the expected power law $\propto t_{obs}$ from the finite size theory for first order transitions. More details are given in the text.

J. Stat. Mech. (2011) P12011

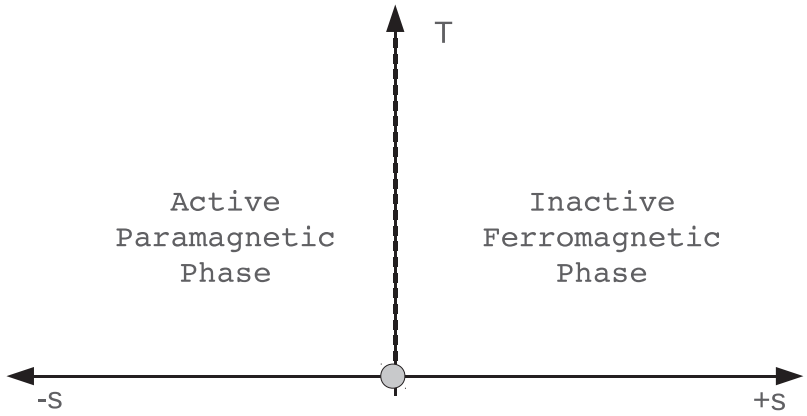

Figure 10. Phase diagram of the Ising chain with Kawasaki dynamics. The dashed line for $s = 0$ represents the points of a first order phase transition between the indicated phases.

in this phase tends to this characteristic value, and consequently the activity is of the same order. This behaviour shows that the inactive phase is a ferromagnet, where the lattice phase separates into two domains, one consisting of up spins and the other of down spins. Such a state will have zero activity in the thermodynamic limit.

We have performed the same analysis for other temperatures, and we conclude that this first order dynamical transition between a paramagnetic/active phase and a ferromagnetic/inactive phase at $s_c = 0$ is present for all temperatures considered ($T = 1$–3). At low temperatures, the accessibility of the transition becomes more difficult because the value of the activity will be much smaller at lower temperatures and it will be zero in the inactive phase, so that the difference between the two phases is too small to resolve. In the limit $T \to 0$ the discontinuity disappears and the transition ends in the point $s = 0, T = 0$. Once again, this is analogous to what occurs in kinetically constrained models [3, 4].

Figure 10 presents the phase diagram that summarizes the result discussed above. This phase diagram for the Ising chain using Kawasaki dynamics should be compared to figure 1 illustrating the Glauber dynamics. These diagrams suggest a very different phase behaviour for models A and B. Models B only exhibit a dynamic phase transition at $s = 0$ between two dynamic asymmetric phases, one is an active paramagnet and the other is an inactive ferromagnet. This first order transition is driven by the biasing field s. For models A, there is a surface of first order lines, between two symmetric ferromagnetic phases, and it is driven by the magnetic field. The surface ends in a critical line in the 2d Ising universality at $s \neq 0$.

5. Conclusions

In this paper we have considered how the dynamical phase behaviour relates to the thermodynamics in the context of the one-dimensional Ising model. We have studied s-ensembles of trajectories [2]–[4], [9] by means of path sampling simulation methods for both Glauber and Kawasaki dynamics. We have both confirmed the analytic predictions

J. Stat. Mech. (2011) P12011

of [17] for Glauber dynamics, and extended the space–time phase diagram to the case of non-zero magnetic field. Our results show an intimate relation between thermodynamic and dynamic phases, but this relation depends on the details of the dynamical rules. For both Glauber and Kawasaki dynamics we show that the paramagnet (which is the stable thermodynamic phase for all $T > 0$ in one dimension) has a counterpart dynamical phase of high activity. While thermodynamically unstable, the static ferromagnetic phase corresponds dynamically to a phase of low activity, and by biasing ensembles of trajectories via the counting field s it is possible to go through a dynamic/non-equilibrium phase transition between the active paramagnetic and the low-activity ferromagnetic phases. In the case of Glauber dynamics, as predicted in [17], this transition is second order and in the 2d Ising model universality class, a fact that we verified numerically by detailed finite size (and time) scaling. Furthermore, with the inclusion of a magnetic field h we were able to show that the area below the line of critical points in the T–s plane at $h = 0$ is actually a surface of first order transitions between low-activity ferromagnetic phases of positive or negative overall magnetization. This is a very interesting example of dimensional reduction: ensembles of trajectories of the 1d Glauber Ising model have statistical properties similar to ensembles of configurations of the equilibrium 2d Ising model.

We also considered the 1d Ising model under Kawasaki dynamics. In this case the transition line between active/paramagnet and inactive/ferromagnet lies on the $s = 0$ axis, a situation analogous to that of kinetically constrained models of glasses [3, 4]. This can be understood by the fact that under Kawasaki dynamics spin exchange leads to transitions in terms of domain walls where there is at least one domain wall present either before or after the transition; the presence of this persistent domain wall plays the role of a kinetic constraint.

The aim of this paper was to shed light on the connection between structural or thermodynamic phase structure and space–time or dynamic phase structure as revealed by the large-deviation method of trajectories. The natural next, and more challenging, step in this programme will be to perform a similar analysis on prototypical systems which display thermodynamic transitions at non-zero temperatures, such as the 2d Ising model.

Acknowledgments

We wish to thank Robert Jack and Frédéric van Wijland for helpful suggestions and comments. The authors are also grateful to the Argentinian Science Agency CONICET and the British Council France Alliance Project 09.013 for their financial support.

References

[1] Merolle M, Garrahan J P and Chandler D, 2005 *Proc. Nat. Acad. Sci.* **102** 10837
[2] Lecomte V, Appert-Rolland C and van Wijland F, 2007 *J. Stat. Phys.* **127** 51
[3] Garrahan J P, Jack R L, Lecomte V, Pitard E, van Duijvendijk K and van Wijland F, 2007 *Phys. Rev. Lett.* **98** 195702
[4] Garrahan J P, Jack R L, Lecomte V, Pitard E, van Duijvendijk K and van Wijland F, 2009 *J. Phys. A: Math. Theor.* **42** 075007
[5] Ruelle D, 2004 *Thermodynamic Formalism* (Cambridge: Cambridge University Press)
[6] Gaspard P, 1998 *Chaos, Scattering and Statistical Mechanics* (Cambridge: Cambridge University Press)
[7] Maes C and Netočný K, 2008 *Europhys. Lett.* **82** 30003
[8] Touchette H, 2009 *Phys. Rep.* **478** 1
[9] Hedges L O, Jack R L, Garrahan J P and Chandler D, 2009 *Science* **323** 1309–13

J. Stat. Mech. (2011) P12011

[10] Lecomte V, Imparato A and van Wijland F, 2010 *Prog. Theor. Phys. Suppl.* **184** 276
[11] Elmatad Y S, Jack R L, Chandler D and Garrahan J P, 2010 *Proc. Nat. Acad. Sci.* **107** 12793–98
[12] Garriga A, Sollich P, Pagonabarraga I and Ritort F, 2005 *Phys. Rev.* E **72** 056114
[13] Kob W and Binder K, 2005 *Glassy Materials and Disordered Solids: An Introduction to Their Statistical Mechanics* (Singapore: World Scientific)
[14] Bodineau T, Derrida B, Lecomte V and van Wijland F, 2008 *J. Stat. Phys.* **133** 1013–31
[15] van Duijvendijk K, Jack R L and van Wijland F, 2010 *Phys. Rev.* E **81** 011110
[16] Jack R L and Garrahan J P, 2010 *Phys. Rev.* E **81** 011111
[17] Jack R L and Sollich P, 2010 *Prog. Theor. Phys. Suppl.* **184** 304–17
[18] Dellago C, Bolhuis P G and Geissler P L, 2003 *Adv. Chem. Phys.* **123** 1–78
[19] Levitov L S, Lee H and Lesovik G B, 1996 *J. Math. Phys.* **37** 4845
[20] Glauber R, 1963 *J. Math. Phys.* **4** 294
[21] Landau D P and Binder K, 2005 *A Guide to Monte Carlo Simulations in Statistical Physics* (Cambridge: Cambridge University Press)
[22] Sachdev S, 1999 *Quantum Phase Transitions* (Cambridge: Cambridge University Press)
[23] Goldenfeld N, 1992 *Lectures on Phase Transitions and the Renormalization Group* (Oxford: Westview Press)
[24] Newman M E J and Barkema G T, 1999 *Monte Carlo Methods in Statistical Physics* (Oxford: Oxford University Press)
[25] Bray A J, 2002 *Adv. Phys.* **51** 481

J. Stat. Mech. (2011) P12011